



Biosorption of Basic Blue 41 from aqueous solutions by *Posidonia oceanica*: Application of two-parameter and three-parameter isotherm models

L. Brahmi, F. Kaouah*, T. Berrama, S. Boumaza, Z. Bendjama

Laboratoire des sciences de génie des procédés industriels, Faculté de Génie Mécanique et de Génie des Procédés, USTHB, BP 32, El-Alia, 16111 Bab-Ezzouar, Alger (Algérie), Tel. +213 666 474 025; email: lamiabr12@hotmail.fr (L. Brahmi), Tel. +213 558 428 259; email: faridakaouah@yahoo.fr (F. Kaouah), Tel. +213 553 979 481; email: tarek_ber@yahoo.fr (T. Berrama), Tel. +213 779 869 856; email: boumzasalim2006@yahoo.fr (S. Boumaza), Tel. +213 556 613 844; email: zbendjama@yahoo.fr (Z. Bendjama)

Received 25 November 2013; Accepted 28 July 2014

ABSTRACT

Batch biosorption experiments were carried out for the removal of basic dye, Basic Blue 41, from aqueous solution using marine biomass *Posidonia oceanica*. A series of assays were undertaken to assess the effect of the systems variables (solution pH, biomass amount, and dye concentration). The highest dye removal yield was achieved at pH 8–11 (i.e., maximum adsorption capacity of 225.48 mg g⁻¹). The minimum sorbent concentration experimentally found to be sufficient to reach the total removal of dye molecules from aqueous solution was 0.4 g L⁻¹. The equilibrium biosorption isotherms and kinetics were investigated. The equilibrium data were fitted using three two-parameter models (Langmuir, Freundlich, and Temkin) and two three-parameter models (Sips and Toth). Langmuir and Sips equations provided the best model for BB41 biosorption data. Kinetic studies indicated that the kinetics of the biosorption of BB41 onto *P. oceanica* follows a pseudo-second-order model. In addition, an exhaustive comparative study was done to situate this marine biomass among other proposed sorbents.

Keywords: Biosorption; *Posidonia oceanica*; Basic Blue (BB) 41; Modeling

1. Introduction

Dyes are synthetic aromatic compounds, which are embodied with various functional groups [1]. To date, there are more than 10,000 dyes available commercially [2]. The annual production of dyes worldwide is around 7 × 10⁵ tons. It is estimated that 5–10% of these chemical compounds are discharged into waste streams by the textile industry [3]. The majority of

these dyes are synthetic origin and toxic in nature with suspected carcinogenic and genotoxic effects [1].

Textile wastewaters offer considerable resistance to biodegradation due to the presence of the dyestuffs, which have a complex chemical structure and are resistant to light, heat, and oxidation agents. The colored dye effluents are considered to be highly toxic to the aquatic life and affect the symbiotic process by disturbing natural equilibrium by reducing photosynthetic activity due to the colorization of the water.

*Corresponding author.

Presented at the 4th Maghreb Conference on Desalination and Water Treatment (CMTDE 2013) 15–18 December 2013, Hammamet, Tunisia

Removal of textile dyes from wastewater is still of a major environmental concern because they are difficult to be removed by the conventional wastewater treatment systems.

Many biological, physical, and chemical methods including coagulation, flocculation, precipitation, filtration, chemical degradation, ozonation, and oxidation have been used for the treatment of dye-containing effluents [4]. These treatments are effective only for small effluent volumes. Therefore, there is a need to find alternative treatments that are effective for large effluent volumes [5].

The adsorption process is being increasingly used due to its high efficiency for pollutant retention. Activated carbon is most widely used adsorbent for the removal of color and the treatment of textile effluents, but it is expensive.

In recent years, there has been an increasing interest in the use of low-cost biosorbent for dye sorption. Thus, locally available materials such as sand [6], cotton fiber [7], canola hull [8], chitosan nanoparticles, cone biomass of *Thuja orientalis* [9], Mediterranean green alga *Enteromorpha* spp. [10], Waste *P. mutilus* biomass [11], clinoptilolite, and amberlite [12] had been successfully used to remove dyes from the aqueous solution.

To the best of our knowledge, no research is currently devoted to addressing the removal of Basic Blue 41 from aqueous solution by *Posidonia oceanica*.

The main focus of this study was to evaluate the biosorption aptitude of low-cost and renewable biomass, *P. oceanica* for the removal of Basic Blue BB41 as model compound for basic dyes.

2. Materials and methods

2.1. Biomass and dye solution preparation

Fresh samples of *P. oceanica* sheets were collected from JIJEL (east coast of Algeria). The samples were rinsed with tap water to remove impurities such as sand and salt absorbed at the surface of the biomass. The washing process was continued until the conductivity value become stable and then dried for 24 h at 80°C.

The dried biomass was grounded by means of a crusher machine. The resulting ground *P. oceanica* biomass with a mean particle size of 200 µm was stored in a desiccator for further use.

The monoazo basic dye, Basic Blue 41 (BB41; CI 11105; CAS 12270-13-2; C₂₀H₂₆N₄O₆S₂; 482.57 g mol⁻¹), furnished by textile Algerian company (Alfaditex, Bejaia, 300 km east Algiers) at 80% purity is the dye used in all experiments. The chemical structure of

BB41 is given in Fig. 1. It is very soluble in water and used in large quantities for dyeing polyacrylonitriles, polyesters, and linear polyamides.

Synthetic dye solution was prepared by dissolving a weighed amount of CI Basic Blue 41 in a precise volume of distilled water.

2.2. Preliminary experiments

2.2.1. Effect of initial pH

Effect of initial pH was investigated at various pH values ranging between 3 and 11. In the experiments, a 0.04 g sample of biomass was added to each 100 mL volume of synthetic dye solution having an initial concentration 100 mg/L in different flasks, for a constant sorption time (1 h), at different pHs. The pHs of the solution was adjusted using HCl and NaOH solutions.

After the sorption step, the solid phase was separated from the dye solution by centrifugation at 3,000 rpm for 5 min. The CI Basic Blue 41 residual concentration was estimated using the spectrophotometry technique at the wavelength of 610 nm.

2.2.2. Effect of sorbent mass

The effect of sorbent mass on the sorbed dye was determined by varying sorbent concentration as 0.1, 0.2, 0.3, 0.4, 0.7, and 0.9 g L⁻¹ in CI Basic Blue 41 solution (100 mg L⁻¹). The obtained samples were shaken at 300 rpm for 1 h. The pH was adjusted at a predetermined optimum solution pH (9).

The biomass amount introduced with the dye solution plays an important role in the percentage of color removal which is expressed by (1):

$$\% \text{ color removal} = [(C_0 - C_e)/C_0] \times 100 \quad (1)$$

where C₀ and C_e are the initial and equilibrium liquid-phase concentrations of BB41 respectively (mg L⁻¹).

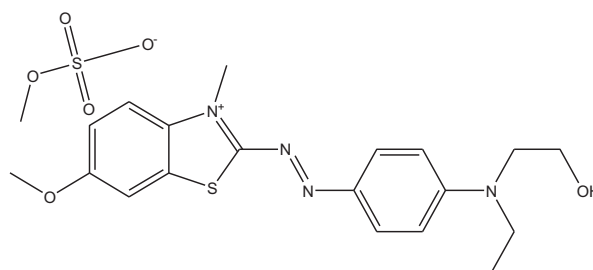


Fig. 1. Chemical structure of BB41.

2.3. Biosorption kinetics–isotherms

Sorption kinetics experiments were carried out at $25 \pm 2^\circ\text{C}$ using five different initial BB41 concentrations, namely 75, 100, 125, 150, and 175 mg L^{-1} . All the kinetics measurements were performed at pH 9, with a maximum contact time of 60 min. The samples were removed at preset time intervals and centrifuged at 3,000 rpm for 5 min.

Biosorption isotherms were carried out by agitating 0.04 g of *P. oceanica* biomass with 100 mL of dye solution concentration varying from 50 to 250 mg L^{-1} at the optimum pH (9) in the thermo-regulated water bath agitated at 300 rpm for the time required to reach the equilibrium state (1 h).

3. Results and discussion

3.1. Surface characterization of novel biosorbent (*P. oceanica*)

To determine the isoelectric point (point of zero charge) of *P. oceanica*, adsorbent was added to potassium nitrate solution (50 mL) in different flask, at different pH values and agitated for 48 h at room temperature [13]. The final pH values of solutions were measured. Final pH of the solution is plotted against initial pH of the solution and shown in Fig. 2.

pH_{PZC} (point of zero charge) for *P. oceanica* is determined as pH 7.24.

3.2. Preliminary study

3.2.1. Effect of initial pH

pH is one of the most important factors controlling adsorption of a dye onto suspended particles. In the present biosorption system, the effect of pH was investigated between 3 and 11 and the result is pre-

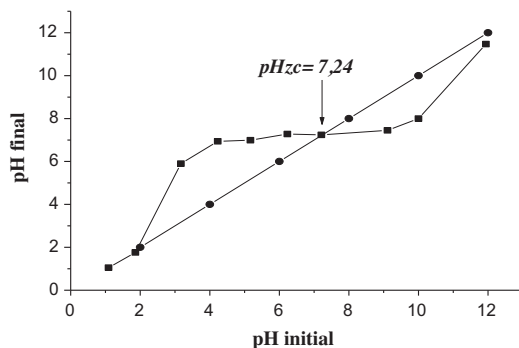


Fig. 2. The isoelectric point determination of *P. oceanica*.

sented in Fig. 3. As shown, the biosorption removal efficiency was minimum at pH 3 (132.90 mg g^{-1}) and increased up to pH 7 (216.49 mg g^{-1}), then remained nearly constant (225.48 mg g^{-1}) over the initial pH of the range 8–11.

The BB41 dye is a cationic with $-\text{NH}_3^+$ group in its structure. At $\text{pH} > 7.24$, an electrostatic attraction exists between positively charged cationic dyes and the negatively charged surface of the adsorbent due to the ionization of functional groups of adsorbent. As the pH of the system decreases, the number of positively charged sites increases. A positively charged site on the adsorbent does not favor the adsorption of cationic dyes due to the electrostatic repulsion [8,10]. Thus, pH 9 was used for further experiments.

3.2.2. Effect of sorbent mass

Fig. 4 shows the % color removal against sorbent concentration (g L^{-1}) of *P. oceanica*. The % color removal increases as the biomass concentration increased. The biosorption removal efficacy values increased from 53.17 to 93.13%, as the biomass dose was increased from 0.1 to 0.9 g L^{-1} . Such a trend is mainly attributed to an increase in the sorptive surface area and the availability of more adsorption sites.

Quite similar tendency was reported for Basic Blue BB41 by a waste containing boron impurity [14].

Moreover, the percentage of removal is stabilized above (0.4 g L^{-1}). This is probably because of the resistance to mass transfer of the dye from bulk liquid to the surface of the solid, which becomes important at high adsorbent loading. For the following experiments, sorbent concentration of *P. oceanica* was set at 0.4 g L^{-1} .

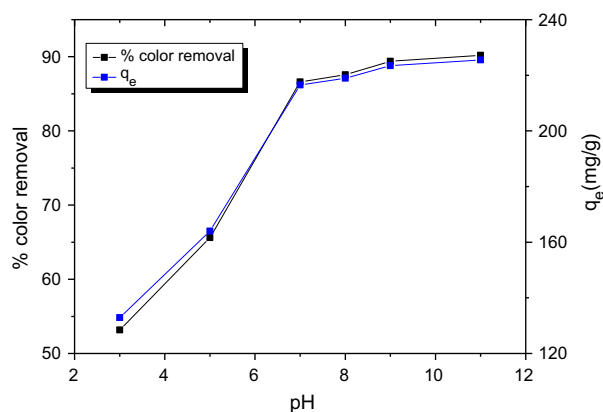


Fig. 3. Effect of solution pH on dye removal.

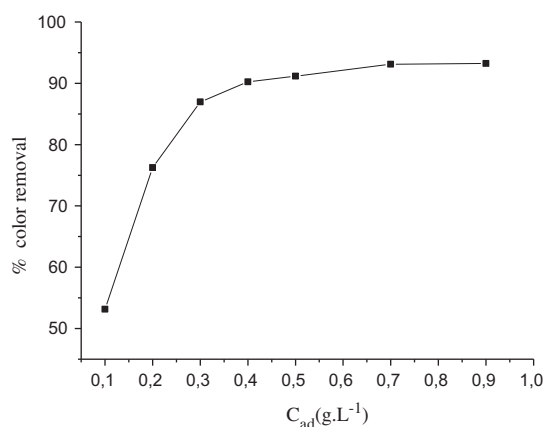


Fig. 4. Effect of biomass amount on the removal of BB41.

3.2.3. Kinetic study

The experimental results of sorption of BB41 on *P. oceanica* at various concentrations are shown in Fig. 5.

The sorption capacity at equilibrium increases from 167.73 to 379.76 mg g⁻¹ with an increase in the initial dye concentration from 75 to 175 mg L⁻¹. Similar results were observed for Basic Blue 69 and Acid Blue 25 by peat [15], for BB41 by dried biomass of Baker's yeast [4].

The increase in the uptake capacity of the sorbent with increasing dye concentration may be due to the increase in sorbate quantity. The variation in the extent of adsorption may also be due to the fact that initially all sites on the surface of the sorbent were vacant and the solute concentration gradient was relatively high. Consequently, the extent of dye uptake decreases significantly with the increase in contact time, which is dependent on the decrease in the number of vacant sites on the surface of dead biomass.

Besides, after the lapse of same time, the remaining vacant surface sites are difficult to occupy due to the

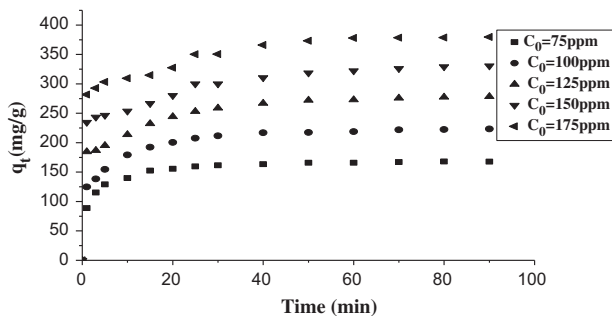


Fig. 5. Effect of initial concentration on the biosorption of BB41 onto *P. oceanica*.

repulsive forces between the solute molecules on the solid surface and the bulk phase, and this trend indicates that the biosorbent saturated at this level [1,16].

Two kinetic models were applied to biosorption kinetic data in order to investigate the behavior of adsorption process of dye onto *P. oceanica*. These models are the pseudo-first-order and pseudo-second-order.

The pseudo-first-order model is given as [17] (2):

$$\log(q_e - q_t) = \log q_e - \left(\frac{K_1}{2,303}\right)t \quad (2)$$

where q_e and q_t are the amount adsorbed (mg g⁻¹) at equilibrium and time t (min), respectively, and K_1 is the pseudo-first-order rate constant of dye (min⁻¹). The values K_1 at different concentrations were calculated from the slopes of the respective linear plots of $\log(q_e - q_t)$ vs. time (Fig. 6) and are tabulated in Table 1. Although the correlation coefficients were higher than 0.93, the calculated $q_{e,cal}$ values do not agree with the experimental value. The results indicated that the biosorption of BB41 onto *P. oceanica* does not follow the pseudo-first-order kinetics.

Kinetic data were further examined with the pseudo-second-order model. If pseudo-second-order kinetics is applicable, the plot of t/q_t vs. time should show a linear relationship. The second-order kinetic model is expressed as follows [18] (3):

$$\frac{t}{q_t} = \frac{1}{K_2 q_e^2} + \frac{1}{q_e} t \quad (3)$$

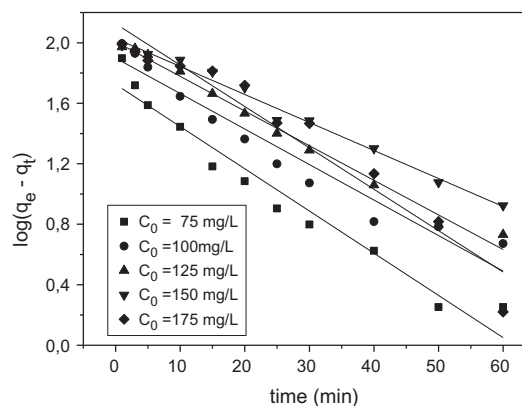


Fig. 6. Pseudo-first-order plots kinetic for biosorption of BB41 onto PO at various concentrations.

Table 1
Kinetic parameters for biosorption of BB41 onto PO at various concentrations

C_0 (mg L ⁻¹)	$q_{e,exp}$ (mg g ⁻¹)	$q_{e,cal}$ (mg g ⁻¹)	K_1 (min ⁻¹)	R^2	$q_{e,cal}$ (mg g ⁻¹)	K_2 (mg g ⁻¹ min ^{-1/2})	R^2
75	167,727	53,078	0.064	0.9514	170,068	0.0042	0.9997
100	223,460	79,242	0.054	0.9413	226,757	0.0023	0.9994
125	278,464	101,587	0.053	0.9894	283,286	0.0017	0.9989
150	330,591	106,770	0.043	0.9868	334,448	0.0013	0.9982
175	379,760	133,564	0.063	0.9375	386,100	0.0014	0.9987

where K_2 is the rate constant of the pseudo-second-order equation (g mg⁻¹ min⁻¹).

The straight-line plots of t/q_t vs. time (Fig. 7) have been used to obtain the rate parameters. The values of K_2 and correlation coefficients R^2 of the dye solutions at different concentrations were calculated from these plots (Table 1). The linear plots of t/q_t vs. time show good agreement with the experimental data from the second-order kinetic model. The correlation coefficients (R^2) were higher than 0.998. The calculated q_e values agree very well with the experimental data. These results indicate that the biosorption of BB41 onto *P. oceanica* obeys pseudo-second-order kinetics.

3.3. Biosorption isotherms

In order to optimize the design of an adsorption system for dye removal, it is important to establish the most appropriate correlation for the equilibrium curves. These equilibrium adsorption capacity curves can be obtained by measuring the adsorption isotherm of basic dyes onto adsorbent. Five different models of sorption isotherms including Langmuir, Freundlich, Temkin, Sips, and Toth have been tested in the present study.

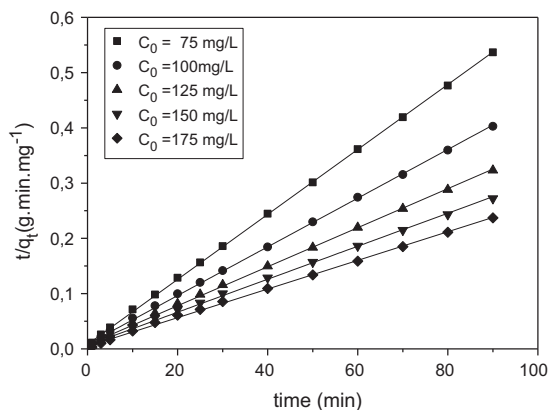


Fig. 7. Pseudo-second-order kinetic biosorption of BB41 onto PO at various concentrations.

3.3.1. Two-parameter models

- The *Langmuir* sorption isotherm, proposed in 1918, assumes that the adsorption takes place at specific homogeneous sites within the adsorption and has found successful application to many sorption processes of monolayer adsorption. The Langmuir isotherm can be written in the form (4):

$$q_e = \frac{q_{max} k_L C_e}{1 + k_L C_e} \quad (4)$$

where q_e is the equilibrium sorbate concentration on the biosorbent (mg g⁻¹), q_{max} (mg g⁻¹) is the maximum biosorption capacity, and k_L (L mg⁻¹) is the biosorption equilibrium constant better known as the Langmuir constant that quantitatively reflects the affinity between the sorbate and the biosorbent.

- The *Freundlich* isotherm is an empirical equation employed to describe heterogeneous systems. It is given by (5):

$$q_e = K_F C_e^{1/n} \quad (5)$$

where K_F [(mg g⁻¹) (L g⁻¹)^{1/n}] is the Freundlich constant related to sorption capacity, and n is the heterogeneity factor.

- The *Temkin* model deals with the heat of adsorption and the involved sorbent/sorbate interactions. Its main assumption is the uniformity in the distribution of binding energies up to some maximum binding energy. The equation of the Temkin model is presented by (6):

$$q_e = \frac{RT}{b} \ln(a_T C_e) \quad (6)$$

where a_T (L g⁻¹) and b (J mol⁻¹) are the Temkin constants.

3.3.2. Three-parameter models

- The *Sips* isotherm has the following form (7):

$$q_e = q_{max} \frac{K_s C_e^{n_s}}{1 + K_s C_e^{n_s}} \tag{7}$$

where K_s is the Sips equilibrium constant ($L\ mg^{-1})^{n_s}$, and n_s is the Sips model exponent.

At low sorbate concentrations, it effectively reduces to the Freundlich isotherm, while at high sorbate concentrations, it predicts monolayer adsorption capacity characteristic of the Langmuir isotherm [19].

- The *Toth* isotherm derived from potential theory has proven useful in describing sorption in heterogeneous systems. It assumes an asymmetrical quasi-Gaussian energy distribution, and most sites have sorption energy less than the mean value [20]. It can be represented as [21] (8):

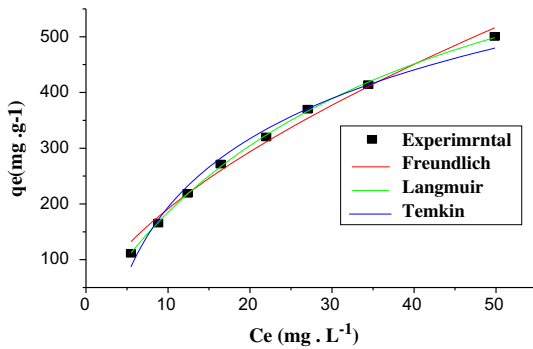


Fig. 8. Comparison of different two-parameter models for BB41 biosorption onto *P. oceanica*.

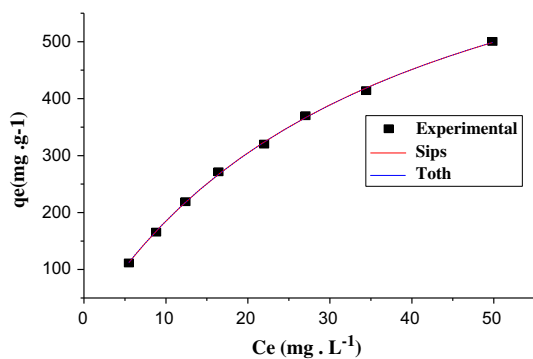


Fig. 9. Comparison of different three-parameter models for BB41 biosorption onto *P. oceanica*.

Table 2

Isotherm constants of two-parameter and three-parameter models for BB41 biosorption onto *P. oceanica*

Langmuir model	q_{max} ($mg\ g^{-1}$)	868.36
	k_L ($L\ mg^{-1}$)	0.027
	R^2	0.999
	χ^2	0.2351
Freundlich model	K_F [$(mg\ g^{-1}) (L\ g^{-1})^{1/n}$]	46.24
	n	1.62
	R^2	0.989
	χ^2	6.0876
Temkin model	b ($J\ mol^{-1}$)	13.93
	a_T ($L\ g^{-1}$)	0.298
	R^2	0.987
	χ^2	9.3171
Sips model	q_{max} ($mg\ g^{-1}$)	868.34
	K_s ($L\ mg^{-1})^{n_s}$	0.02704
	n_s	1.00004
	R^2	0.99937
	χ^2	0.2351
Toth model	q_{max} ($mg\ g^{-1}$)	882.46
	b_T ($L\ mg^{-1}$)	0.26841
	n_T	0.98223
	R^2	0.99938
	χ^2	0.2418

$$q_e = q_{max} \frac{b_T C_e}{(1 + (b_T C_e)^{n_T})^{1/n_T}} \tag{8}$$

where b_T ($L\ mg^{-1}$) and n_T are Toth constants.

All the model parameters were evaluated by non-linear regression using the ORIGIN 8.6 software. The fitted data for Langmuir, Freundlich, Temkin, Sips, and Toth isotherm models are shown in Figs. 8 and 9.

The correlation coefficients and the chi-square test are used to measure the goodness-of-fit. The chi-square test is defined as (9):

Table 3

Separation factor, R_L , calculated for BB41 biosorption onto *P. oceanica*

Initial dye concentration ($mg\ L^{-1}$)	R_L
50	0.425
75	0.33
100	0.27
125	0.228
150	0.198
175	0.175
200	0.156
250	0.129

Table 4

Comparison of biosorption capacity between *P. oceanica* and other studied sorbents for cationic textile dye removal

Sorbents	Textile dyes	pH	T (°C)	q_{max} (mg g ⁻¹)	References
<i>Posidonia oceanica</i>	Basic Blue 41	9	25	868.36	This study
Waste <i>P. mutilus</i>	Basic Blue 41	8	30	111.00	[11]
<i>Accharomyces cerevisiae</i>	Basic Blue 41	9	30	212.77	[4]
<i>Clinoptilolite</i>	Basic Yellow 28	6–6.5	20	59.60	[12]
Peat	Basic Blue 69	–	40	253.00	[15]
<i>Enteromorpha spp</i>	Methylene blue	6	30	270.27	[10]
Canola hull	Basic Red 46 and Basic Violet 16	8	20	49.02 25.00	[8]

$$\chi^2 = \sum \frac{(q_{e,meas} - q_{e,cal})^2}{q_{e,cal}} \quad (9)$$

where $q_{e,meas}$ and $q_{e,cal}$ (mg g⁻¹) are the experimental and calculated values of the equilibrium adsorbate concentration in the solid phase. The model is considered most suitable to satisfactorily describe the biosorption process if it provides the highest R^2 and the lowest error calculation values χ^2 . The different isotherm parameters along with R^2 and χ^2 values are given, respectively, in Table 2.

High R^2 (0.999) value and low χ^2 (0.2351) value (Table 2) for the Langmuir model indicate that the biosorption of BB41 onto *P. oceanica* follows the Langmuir model. The excellent fit of the Langmuir isotherm to the experimental biosorption data confirms that the biosorption is monolayer; biosorption of each molecule has equal activation energy and that sorbate–sorbate interaction is negligible.

On the basis of correlation coefficients and chi-square test (Table 2), the experimental data were better described by the Sips model followed by Toth ($R^2 = 0.999$ for both models). Besides, the Sips constant ($n_s = 1.00004$) confirms the fact that the isotherm is more approaching the Langmuir than the Freundlich isotherm. It effectively reduces to a Langmuir isotherm ($n_s \cong 1$) [22–24].

The essential features of a Langmuir isotherm can be expressed in terms of a dimensionless constant separation factor or equilibrium parameter, R_L which is defined as (10):

$$R_L = \frac{1}{1 + k_L C_0} \quad (10)$$

The parameter R_L indicates that the shape of the isotherm. If the R_L values are higher than 1, it indicates

unfavorable adsorption. If the R_L values are 1, it indicates linear adsorption. R_L values between 0 and 1 indicate favorable adsorption. If the R_L values are zero, it indicates irreversible adsorption.

The calculated R_L values, shown in Table 3, were all in the range of 0–1, which confirms the favorable adsorption of the biosorption process in the studied experimental conditions.

3.3.3. Comparison with other biosorbents

On the other hand, in order to situate our novel biosorbent among those used to remove cationic textile dyes from aqueous solutions, a comparison based on the Langmuir saturation capacity, q_{max} , was carried out. The results, illustrated in Table 4, showed that the *P. oceanica* could be considered as a promising biomaterial to remove textile dyes when compared to other biological materials and even to different kinds of activated carbons.

4. Conclusion

BB41 removal from the aqueous solution through biosorption onto *P. oceanica* was investigated in the present study. The biosorption capacity was estimated as a function of initial pH, initial dye concentrations, and biosorbent dosage. The kinetic study of BB41 on *P. oceanica* was performed based on pseudo-first-order and pseudo-second-order. The data indicate that the adsorption kinetics follow the pseudo-second-order rate. The equilibrium sorption phenomena were found to be well described by both Langmuir and Sips models. In both cases, such modeling behavior confirms the monolayer coverage of BB41 molecules onto energetically *P. oceanica* surface. The comparison of the biosorption aptitude between *P. oceanica* and other biosorbent materials indicated that the experimented Mediterranean biomass showed a very good biosorption capacity toward the tested basic dye.

References

- [1] B. Noroozi, G.A. Sorial, H. Bahrami, M. Arami, Equilibrium and kinetic adsorption study of a cationic dye by a natural adsorbent-silkworm pupa, *J. Hazard. Mater.* 139 (2007) 167–174.
- [2] R. Gong, Y. Sun, J. Chen, H. Liu, C. Yang, Effect of chemical modification on dye adsorption capacity of peanut hull, *Dyes Pigm.* 67(3) (2005) 175–181.
- [3] M.C. Ncibi, B. Mahjoub, M. Seffen, Studies on the biosorption of textile dyes from aqueous solutions using *Posidonia oceanica* (L.) leaf sheath fibers, *Adsorpt. Sci. Tech.* 24(6) (2007) 461–473.
- [4] J.Y. Farah, N.Sh. El-Gendy, L.A. Farahat, Biosorption of Astrazone Blue basic dye from an aqueous solution using dried biomass of Baker's yeast, *J. Hazard. Mater.* 148(1–2) (2007) 402–408.
- [5] I. Guezguez, S. Dridi-Dhaouadi, F. Mhenni, Sorption of Yellow 59 on *Posidonia oceanica*, a non-conventional biosorbent: Comparison with activated carbons, *Ind. Crops Prod.* 29(1) (2009) 197–204.
- [6] S.B. Bukallah, M.A. Rauf, S.S. Alali, Removal of methylene blue from aqueous solution by adsorption on sand, *Dyes Pigm.* 74(1) (2007) 85–87.
- [7] M. Saleem, T. Pirzada, R. Qadeer, Sorption of acid violet 17 and direct red 80 dyes on cotton fiber from aqueous solutions, *Colloids Surf., A* 292 (2007) 246–250.
- [8] N.M. Mahmoodi, M. Arami, H. Bahrami, S. Khorramfar, Novel biosorbent (*Canola* hull): Surface characterization and dye removal ability at different cationic dye concentrations, *Desalination* 264 (2010) 134–142.
- [9] A. Tamer, A.S. Ozcan, S. Tunalı, A. Ozcan, Biosorption of a textile dye (Acid Blue 40) by cone biomass of *Thuja orientalis*: Estimation of equilibrium, thermodynamic and kinetic parameters, *Bioresour. Technol.* 99 (2008) 3057–3065.
- [10] M.C. Ncibi, A.M. Ben Hamissa, A. Fathallah, M.H. Kortas, T. Baklouti, B. Mahjoub, M. Seffen, Biosorptive uptake of methylene blue using Mediterranean green alga *Enteromorpha* spp. *J. Hazard. Mater.* 170 (2009) 1050–1055.
- [11] N. Yeddou-Mezenner, Kinetics and mechanism of dye biosorption onto an untreated antibiotic waste, *Desalination* 262 (2010) 251–259.
- [12] J. Yener, T. Kopac, G. Dogu, T. Dogu, Adsorption of Basic Yellow 28 from aqueous solutions with clinoptilolite and amberlite, *J. Colloid Interface Sci.* 294 (2006) 255–264.
- [13] S.K. Mishra, S.B. Kanungo, Rajeev, Adsorption of sodium dodecyl benzenesulfonate onto coal, *J. Colloid Interface Sci.* 267 (2003) 42–48.
- [14] A. Necip, A. Olgun, Removal of basic and acid dyes from aqueous solutions by a waste containing boron impurity, *Desalination* 249 (2009) 109–115.
- [15] Y.S. Ho, C.T. Huang, H.W. Huang, Equilibrium sorption isotherm for metal ions on tree fern, *Process Biochem.* 37 (2002) 1421–1430.
- [16] O. Hamdaoui, F. Saoudi, M. Chiha, E. Naffrechoux, Sorption of malachite green by a novel sorbent, dead leaves of plane tree: Equilibrium and kinetic modeling, *Chem. Eng. J.* 143 (2008) 73–84.
- [17] S. Lagergreem, Zur theorie der sogenannten adsorption gelöster stoffe (About theory of so-called adsorption of soluble substances), *Kungliga Svenska Vetenskapsakademiens Handlingar* 24(4) (1898) 1–39.
- [18] Y.S. Ho, G. McKay, Kinetics model for lead (II) sorption onto peat, *Adsorpt. Sci. Technol.* 16 (1998) 243–255.
- [19] R. Sips, On the structure of a catalyst surface, *J. Chem. Phys.* 16 (1948) 490–495.
- [20] Y.S. Ho, G. McKay, Kinetic Models for the sorption of dye from aqueous solution by wood, *Process Saf. Environ. Prot.* 76 (1998) 183–191.
- [21] J. Toth, *Acta Chim. Acad. Sci., Hungaricae* 69 (1971) 311–317.
- [22] L. Abramian, H. El-Rassy, Adsorption kinetics and thermodynamics of azo-dye Orange II onto highly porous titania aerogel, *Chem. Eng. J.* 150 (2009) 403–410.
- [23] L.S. Chan, W.H. Cheung, S.J. Allen, G. McKay, Separation of acid-dyes mixture by bamboo derived active carbon, *Sep. Purif. Technol.* 67 (2009) 166–172.
- [24] L.G. da Silva, R. Ruggiero, P.de M. Gontijo, R.B. Pinto, B. Royer, E.C. Lima, T.H.M. Fernandes, T. Calvete, Adsorption of Brilliant Red 2BE dye from water solutions by a chemically modified sugarcane bagasse lignin, *Chem. Eng. J.* 168 (2011) 620–628.